Available online at www.sciencedirect.com
ScienceDirect
Journal of Power Sources 171 (2007) 789–792
JOURNAL OF POWER SOURCES
www.elsevier.com/locate/jpowsour

Short communication

Characterisation of Ni-cermets SOFCs with varying anode densities

V.A.C. Haanappel *, J. Mertens, J. Malzbender

Institute for Energy Research, Forschungszentrum Jülich, D-52425 Jülich, Germany

Received 15 March 2007; received in revised form 29 May 2007; accepted 3 June 2007
Available online 13 June 2007

Abstract

Mechanical reliability is a critical parameter for both the assembling and long-term operation of solid oxide fuel cells (SOFCs). The mechanical robustness of the SOFCs depends critically on the strength of the anode substrate. To enhance the mechanical strength, the density of the anode substrate was increased. Three variations were chosen in addition to the standard-type SOFCs (4.7 g cm^{-3}): +5% (4.9 g cm^{-3}), +10% (5.1 g cm^{-3}) and +15% (5.3 g cm^{-3}). These SOFCs were characterised with respect to their bending strength, transport parameters, and electrochemical performance.

The experimental results showed that the mechanical strength of the anodes can be improved. The electrochemical performance was not detrimentally influenced.

Keywords: SOFC; Anode; Anode-supported; Mechanical strength; Electrochemical performance

1. Introduction

Solid oxide fuel cells (SOFCs) with high power densities [1–4] have already been used for stacks with various designs developed at Forschungszentrum Jülich [5]. The more recent designs are based on the use of relatively thin sheet metal with the aim of making the SOFC stack systems lighter and more compact: a weight reduction between 80 and 90% is potentially achievable, which has obvious advantages for use as automotive power units. With such a design, the anode substrate cells need to exhibit sufficient strength to withstand handling during stack assembly and operation under stationary and thermal cycling conditions. The effect of varying the porous ceramic anode substrate density is one means of potentially realising such an increase in the mechanical strength of the cells. The SOFCs are characterised with respect to their bending strength, transport parameters, and electrochemical performance.

2. Experimental

FZJ-type anode-supported single cells with dimensions of 50 mm × 50 mm were used for electrochemical measurements and are based on an anode substrate (thickness: ∼1 mm), an anode functional layer (AFL) (thickness: 8 μm) and an electrolyte (thickness: ∼10 μm). The anode substrate consists of a porous composite of NiO and zirconia stabilised with 8 mol% yttria (8YSZ). In addition to the standard density of the anode substrate in the oxidation state, which is set at 100% (4.7 g cm^{-3}), also higher densities of the substrate were produced, i.e. +5% (4.9 g cm^{-3}), +10% (5.1 g cm^{-3}), and +15% (5.3 g cm^{-3}). Regarding bending strength tests, the dimensions of the samples were about 24 mm × 24 mm. In this case, the samples consisted only of an anode substrate, an anode functional layer, and an electrolyte. The processing conditions were similar to those for the 50 mm × 50 mm samples.

The $La_{0.65}Sr_{0.3}MnO_3$/YSZ cathode functional layer, with a thickness of 10 μm, is based on a mass ratio of 50/50. The thickness of the cathode current collector layer type $La_{0.65}Sr_{0.3}MnO_3$ was between 70 and 80 μm. Both layers were applied by screen printing, followed by co-firing at 1100 °C. The area of both layers was 40 mm × 40 mm. More information on the production route can be found elsewhere [1–10].

Electrochemical measurements of single cells were performed in an alumina test housing placed inside the furnace. In order to obtain sufficient electronic contact between the cell and the electronic devices, at the anode side a Ni mesh was used and at the cathode side a Pt mesh. More information on the experimental method is given in references [1–4].

Determination of transport parameters of the fuel gas in porous media is based on the mean transport pore model

* Corresponding author. Tel.: +49 2461 614656; fax: +49 2461 616770.
E-mail address: v.haanappel@fz-juelich.de (V.A.C. Haanappel).

0378-7753/$ – see front matter © 2007 Elsevier B.V. All rights reserved.
doi:10.1016/j.jpowsour.2007.06.006

(MTPM) [11–13]. The MTPM assumes that the decisive part of the gas transport takes place in pores which are regarded as cylindrical capillaries. The main model parameters to be calculated are the mean radius $\langle r\rangle$ of the capillaries, the mean of the square of the radius of the transport pores $\langle r^2\rangle$ and the factor $\psi = \varepsilon_T/\tau$, which is the ratio of the porosity of the transport pores ε_T and the tortuosity factor τ. The diffusion processes of gases are described by the modified Maxwell-Stefan equation [12]. For more information on the testing unit and test performance, see references [14,15].

To assess the mechanical stability of SOFCs bending strength tests with small samples (20 specimens per set) were carried out in accordance with the European Standard EN 1288-1 "Glass in Building. Determination of the Bending Strength of Glass. Part 1: Fundamentals of Testing Glass". This document describes in detail the procedure for determining the bending strength of monolithic glass using the so-called ring-on-ring test. This procedure was used here to determine the bending strength of the anode substrate. Although this approach is only valid for isotropic materials, it can also be used for the underlying anode substrates with a thickness of about 1 mm, since the thin electrolyte, which has only a minor effect on the strength, can be neglected [16–18]. Since the test procedure was used to determine the bending the strength of the anode substrate, and the thin electrolyte (10 μm) has only a minor effect on the strength, specimens including a cathode layer with a thickness of about 80 μm, thus much thicker than the electrolyte layer, cannot be used. In that case, the presence of the cathode layer could not be neglected anymore. The strength in the ring-on-ring method [16] can be calculated from:

$$\sigma_B = \frac{3(1+\mu)}{2\pi}\left[\ln\frac{r_2}{r_1} + \frac{(1-\mu)}{(1+\mu)}\frac{r_2^2 - r_1^2}{2r_3^2}\right]\frac{F}{h^2}$$

where σ_B is the bending strength (MPa), μ the Poisson ratio, r_1 the radius of the inner ring, r_2 the radius of the outer ring, r_3 the radius for round samples, F the applied force, and h is the thickness of the sample.

For the square samples used an effective radius $r_{3,\text{eff}}$ has to be substituted for r_3 defined as:

$$r_{3,\text{eff}} = \frac{(1+\sqrt{2})}{2}\frac{L}{2} \approx 0.60L$$

Failure characterisation usually relies on Weibull statistics. From the fracture stress values the associated characteristic strength and Weibull modulus are determined using the so-called maximum likelihood method as outlined in DIN EN 843-5. These two parameters are used to assess the potential effect of a density variation.

The stoichiometry of the various powders was verified by optical spectroscopy (ICP-OES) and the phase purity by X-ray diffraction (Siemens D 500). Grain size distribution measurements of powders were carried out by a Fritsch Analysette 22 with software version 1.8.0. SEM analysis was performed using a Gemini electron microscope (LEO 1530).

3. Results and discussion

The current densities at 700 mV and the area-specific resistance between 650 and 900 °C of the cells are listed in Table 1. Calculations of the current density at 700 mV at exact temperatures are based on inter- or extrapolation (for $I > 1.25$ A cm^{-2}) using a 2nd or 3rd order polynomial function. Calculations of the area-specific resistance are based on linear regression or linear extrapolation of the current–voltage curves at 700 mV. From this table it is clear that the area-specific resistance and thus the current density were not obviously affected by gravimetric variations in the density of the anode. Fig. 1 shows, as an example, the current–voltage curves for a single cell with a deviation of +10% from the standard density of the anode.

The transport parameters characterising the porous structure of the anode according to the mean transport pore model are (a) the $\langle r\Psi\rangle$ factor; (b) the $\langle r^2\Psi\rangle$ factor; (c) the Ψ factor, which can be considered as the ratio of the porosity of the transport pores and the tortuosity factor; (d) $\langle r\rangle$ the mean radius of the transport pores. These parameters were obtained by numerical solutions.

Table 1
Average values of calculated current densities (CD) and area-specific resistance (ASR) at 700 mV for LSM-type single cells with variations in the substrate density (A cm^{-2}, mΩ cm^2, both at 700 mV) between 650 and 900 °C

Temperature (°C)	Standard	Standard + 5%	Standard + 10%	Standard + 15%
Current density (A cm^{-2})				
900	2.30 ± 0.10	1.94 ± 0.05	2.01 ± 0.02	2.07 ± 0.01
850	1.95 ± 0.04	1.76 ± 0.03	1.81 ± 0.02	1.84 ± 0.01
800	1.49 ± 0.02	1.43 ± 0.03	1.46 ± 0.01	1.46 ± 0.01
750	0.99 ± 0.01	1.02 ± 0.02	1.03 ± 0.01	1.01 ± 0.03
700	0.59 ± 0.01	0.63 ± 0.02	0.63 ± 0.02	0.62 ± 0.03
650	0.33 ± 0.01	0.35 ± 0.01	0.34 ± 0.01	0.33 ± 0.01
Area-specific resistance (mΩ cm^2)				
900	127 ± 5	147 ± 2	150 ± 2	152 ± 2
850	151 ± 3	165 ± 2	167 ± 2	167 ± 2
800	190 ± 2	203 ± 2	200 ± 2	202 ± 2
750	258 ± 6	300 ± 7	288 ± 6	278 ± 5
700	423 ± 10	462 ± 11	443 ± 10	437 ± 10
650	750 ± 21	834 ± 22	804 ± 17	760 ± 19

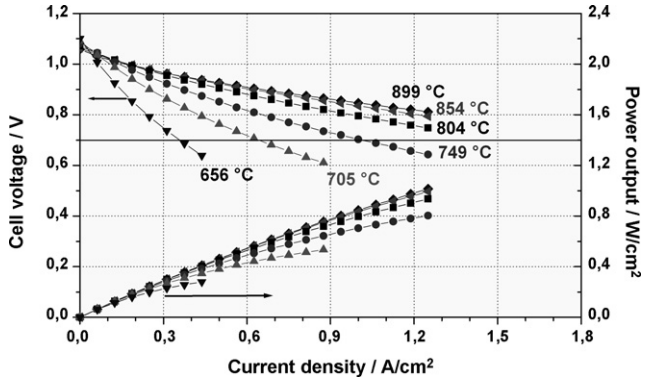

Fig. 1. Current–voltage and power output curves for a 16 cm^2 single cell with LSM cathode and including an anode with a deviation of +10% from the standard density. Fuel gas: H_2 (3% H_2O) = 1000 ml min^{-1}; oxidant: air = 1000 ml min^{-1}.

The transport parameters $\langle r\Psi \rangle$ and $\langle r^2\Psi \rangle$ derived from the permeation measurements are shown in Fig. 2. It appears that these factors decrease with increasing anode density indicating a lower permeability for the gases used. This tendency was observed for the anodes in the oxidised as well as in the reduced state, although the absolute values are smaller for the oxidised anode. The mean pore radius of the anode and the Ψ factor, which were calculated from both diffusion and permeation measurements, are shown in Fig. 3. It is clear that the Ψ factor decreases with increasing anode density. The mean pore radius of the different anodes types is not affected within the limits of uncertainty.

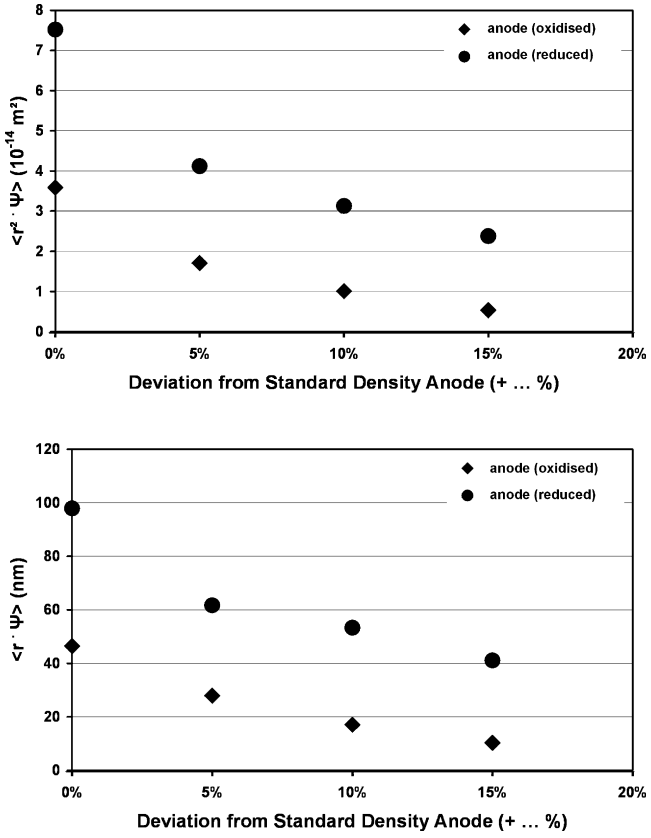

Fig. 2. Transport parameters, related to the permeation measurements from the MTPM model as a function of the deviation from the standard density of the anode: (a) $\langle r^2\Psi \rangle$ factor; (b) $\langle r\Psi \rangle$ factor.

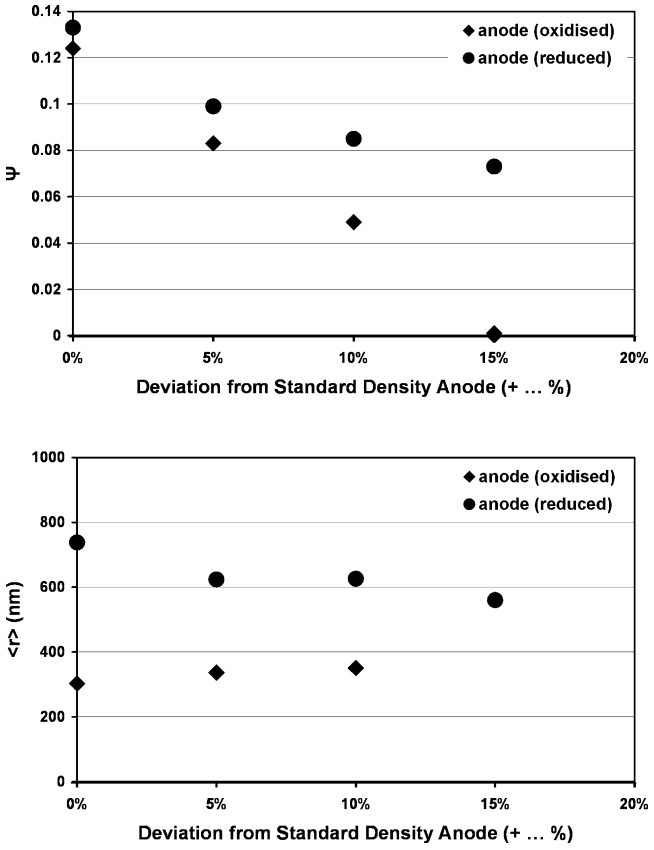

Fig. 3. Transport parameters from the MTPM model and calculated from the permeation and diffusion measurements as a function of the deviation from the standard density of the anode: (a) Ψ factor; (b) mean pore radius $\langle r \rangle$.

The characteristic bending strengths obtained using the ring-on-ring test of samples with different anode substrate densities are given in Table 2. The bending strength increases for the series with a higher density as compared to the standard production. However, no strength difference is measurable between the series with various higher substrate densities. With respect to the Weibull modulus, the values for the +5 and +15% series are only slightly lower. In the case of the series with +10%, the bending strength is slightly higher than that of the series +5 and +15%. However, in this case the slightly lower Weibull modulus potentially results in a higher failure probability.

Table 2
Average values of bending strength and Weibull modulus for a series of single cells including various densities of the anode substrate

Density	Characteristic bending strength (MPa)	Weibull modulus
Standard	70.7 ± 2.4	8.1 ± 2.7
Standard + 5%	88.0 ± 2.4	7.7 ± 1.7
Standard + 10%	90.3 ± 3.3	5.9 ± 1.4
Standard + 15%	88.7 ± 2.1	7.3 ± 1.3

4. Conclusions

Thin anode substrates with a thickness of about 1 mm and higher density were successfully produced for the fabrication of anode-supported cells. The experimental results permit the following conclusions with respect to variations in the substrate density:

- The permeability, given by $\langle r\Psi \rangle$ and $\langle r^2\Psi \rangle$, decreases with increasing gravimetric density of the anode, although the permeability of cells in the oxidised state is always lower than in the reduced state.
- The Ψ-factor decreases with increasing anode density. The effect is always smaller for cells in the oxidised than in the reduced state.
- The mean pore diameter is not measurably affected by density variations, but is always higher for cells with anodes in the reduced state.
- The electrochemical performance is not affected within the limits of uncertainty by variations in the density of the anode.
- The characteristic bending strength is higher for cells with a higher anode density. However, no differences are measurable between the specimen sets with increased density.

Acknowledgements

The authors gratefully acknowledge Ms. M. Andreas for the synthesis of spray-dried cathode powder, Mr. S. Heinz, Ms. Portulidou and Mr. W. Herzhof for the preparation of SOFCs, and Ms. C. Tropartz, Ms. B. Röwekamp and Mr. H. Wesemeyer for performing the electrochemical measurements.

References

[1] J. Mertens, V.A.C. Haanappel, D. Rutenbeck, H.P. Buchkremer, D. Stöver, in: M. Mogensen (Ed.), Proceedings of the Sixth European Solid Oxide Fuel Cells Forum, Lucerne, Switzerland, 28 June–2 July, 2004, pp. 1263–1270.
[2] V.A.C. Haanappel, J. Mertens, D. Rutenbeck, W. Herzhof, D. Sebold, F. Tietz, J. Power Sources 141 (2005) 216–226.
[3] A. Mai, V.A.C. Haanappel, F. Tietz, D. Stöver, in: S.C. Singhal, J. Mizusaki (Eds.), Proceedings of the Ninth International Symposium (15–20 May, 2005, Quebec, Canada) on Solid Oxide Fuel Cells (SOFC IX), PV2005-07: Solid Oxide Fuel Cells IX, The Electrochemical Society Proceedings Series, Pennington, NJ, 2005, pp. 1627–1635.
[4] V.A.C. Haanappel, J. Mertens, A. Mai, in: N.M. Sammes (Ed.), Proceedings of the First European Fuel Cell Technology & Applications Conference, 14–16 December, 2005, Rome, Italy: J. Fuel Cell Sci. Technol. 3 (2006) 263–270.
[5] R. Steinberger-Wilckens, I.C. Vinke, L. Blum, L.G.J. de Haart, J. Remmel, F. Tietz, W.J. Quadakkers, in: M. Mogensen (Ed.), Proceedings of the Sixth European Solid Oxide Fuel Cells Forum, Lucerne, Switzerland, 28 June–2 July, 2004, pp. 11–19.
[6] H.P. Buchkremer, U. Dieckmann, D. Stöver, in: B. Thorstensen (Ed.), Proceedings of the Second European Solid Oxide Fuel Cell Forum, B. European SOFC Forum, Oberrohrdorf, Switzerland, 1996, pp. 221–228.
[7] J.P.P. Huijsmans, F.P.F. Berkel van, G.M. Christie, J. Power Sources 71 (1998) 107–110.
[8] J.W. Yan, Y.G. Lu, Y. Jiang, Y.L. Dong, C.U. Yu, W.Z. Li, J. Electrochem. Soc. 149 (9) (2002) A1132–A1135.
[9] J.W. Erning, T. Hauber, U. Stimming, K. Wipperman, J. Power Sources 61 (1996) 205–211.
[10] L.G.J. de Haart, K. Mayer, U. Stimming, I.C. Vinke, J. Power Sources 71 (1998) 302–305.
[11] P. Fott, S. Petrini, P. Schneider, Collection Czechoslovak Chem. Commun. 48 (1983) 215–227.
[12] D. Arnost, P. Schneider, Chem. Eng. J. 57 (1995) 91–99.
[13] L.B. Rothfeld, AIChE J. 9 (1) (1963) 19–24.
[14] P. Hejtmanek, P. Capek, O. Solcova, P. Schneider, Chem. Papers 54 (4) (2000) 215–220.
[15] J. Mertens, V.A.C. Haanappel, H.P. Buchkremer, J. Fuel Cell Sci. Technol. 3 (4) (2006) 414–421.
[16] European Standard EN 1288-1, Glass in Building—Determination of the Bending Strength of Glass. Part 1: Fundamentals of Testing Glass, 2000.
[17] J. Malzbender, R.W. Steinbrech, L. Singheiser, Ceram. Eng. Sci. Proc. 26 (4) (2005) 294–298.
[18] J. Malzbender, R.W. Steinbrech, Surf. Coat. Technol. 176 (2004) 165–172.